

Abnormal resting-state functional network centrality in patients with high myopia: evidence from a voxel-wise degree centrality analysis

Yu-Xiang Hu¹, Jun-Rong He², Bo Yang³, Xin Huang¹, Yu-Ping Li⁴, Fu-Qing Zhou⁵, Xiao-Xuan Xu¹, Yu-Lin Zhong¹, Jun Wang⁶, Xiao-Rong Wu¹

¹Department of Ophthalmology, the First Affiliated Hospital of Nanchang University, Nanchang 330006, Jiangxi Province, China

²Department of Quality Management Office, the Affiliated Ganzhou Hospital of Nanchang University, Ganzhou 341000, Jiangxi Province, China

³Department of Ophthalmology, Xinjiang People's Hospital, Urumqi 830000, Xinjiang Uygur Autonomous Region, China

⁴Department of Ophthalmology, Dongxiang People's Hospital, Fuzhou 344000, Jiangxi Province, China

⁵Department of Radiology, the First Affiliated Hospital of Nanchang University, Jiangxi Province Medical Imaging Research Institute, Nanchang 330006, Jiangxi Province, China

⁶Second Department of Respiratory Disease, Jiangxi Provincial People's Hospital, Nanchang 330006, Jiangxi Province, China

Co-first authors: Yu-Xiang Hu and Jun-Rong He

Correspondence to: Xiao-Rong Wu. Department of Ophthalmology, the First Affiliated Hospital of Nanchang University, Nanchang 330006, Jiangxi Province, China. wxr98021@126.com; Jun Wang. Second Department of Respiratory Disease, Jiangxi Provincial People's Hospital, Nanchang 330006, Jiangxi Province, China. wangjun5087@163.com

Received: 2018-01-15 Accepted: 2018-09-10

Abstract

• **AIM:** To investigate the functional networks underlying the brain-activity changes of patients with high myopia using the voxel-wise degree centrality (DC) method.

• **METHODS:** In total, 38 patients with high myopia (HM) (17 males and 21 females), whose binocular refractive diopter were -6.00 to -7.00 D, and 38 healthy controls (17 males and 21 females), closely matched in age, sex, and education levels, participated in the study. Spontaneous brain activities were evaluated using the voxel-wise DC method. The receiver operating characteristic curve was measured to distinguish patients with HM from healthy controls. Correlation analysis was used to explore the relationship between the observed mean DC values of the different brain areas and the behavioral performance.

• **RESULTS:** Compared with healthy controls, HM patients had significantly decreased DC values in the right inferior frontal gyrus/insula, right middle frontal gyrus, and right supramarginal/inferior parietal lobule ($P<0.05$). In contrast, HM patients had significantly increased DC values in the right cerebellum posterior lobe, left precentral gyrus/postcentral gyrus, and right middle cingulate gyrus ($P<0.05$). However, no relationship was found between the observed mean DC values of the different brain areas and the behavioral performance ($P>0.05$).

• **CONCLUSION:** HM is associated with abnormalities in many brain regions, which may indicate the neural mechanisms of HM. The altered DC values may be used as a useful biomarker for the brain activity changes in HM patients.

• **KEYWORDS:** high myopia; degree centrality; functional magnetic resonance imaging; resting state

DOI:10.18240/ijo.2018.11.13

Citation: Hu YX, He JR, Yang B, Huang X, Li YP, Zhou FQ, Xu XX, Zhong YL, Wang J, Wu XR. Abnormal resting-state functional network centrality in patients with high myopia: evidence from a voxel-wise degree centrality analysis. *Int J Ophthalmol* 2018;11(11):1814-1820

INTRODUCTION

High myopia (HM) is a very common eye problem characterized by impairment in distance vision. HM has become a global public health problem, and the prevalence of HM will reach up to 9.8% of the world population by 2050^[1]. Furthermore, the prevalence of HM in young Asian adults is higher than in corresponding non-Asian populations^[2]. HM does not only impair vision, but also lead to a variety of eye complications, such as macular complications^[3], choroidal thinning^[4] and retinal detachment^[5]. HM is caused by different kinds of risk factors, such as genetic^[6], educational^[7] and environmental factors^[8]. Currently, the main treatments for HM are laser *in situ* keratomileusis^[9] and implantation of intraocular lens^[10].

Optical coherence tomography (OCT) accurately measures the structure of the eye by using a noninvasive, high-resolution

approach. Malakar *et al*^[11] demonstrated that the HM group showed a thinner retinal nerve fiber layer than the emmetropic eye group applying the OCT method^[11]. Another study suggested that HM patients showed a lower microvessel density of the retinal annular zone than the control group using OCT angiography^[12]. Furthermore, HM might lead to choroidal thinning^[4]. Magnetic resonance imaging (MRI) was applied to assess the eye shape in HM patients^[13], which is correlated with impaired vision^[14]. However, the above-mentioned studies emphasize solely on the pathological changes of ocular trauma in HM. The normal function of the visual system includes the visual pathway of the eye and the visual cortex, which might be affected in HM. However, changes of spontaneous brain activities in HM are less studied.

Abnormal anatomical and functional of the brain with HM patients have been revealed in recent studies. Functional magnetic resonance imaging (fMRI) has been used to assess the brain activities in HM patients, revealing that myopia decreases on the visual cortex activity^[15]. Another study exhibited that HM patients showed increased white matter in the calcarine area compared with emmetropia^[16]. In our previous study, we found that HM patients showed significant amplitude of low-frequency fluctuation changes in many brain regions, which might reflect impairment in language understanding in HM patients^[17]. Moreover, Zhai *et al*^[18] revealed that HM patients were associated with significantly decreased function connectivity in ventral attention and frontoparietal control networks. However, the abovementioned researches focused on alterations of visual cortex or regional brain activity occurred in HM subjects. However, there are limited studies that directly explore the whole-brain network hubs in HM patients. Hubs enable integration of diverse informational sources and serve to balance opposing pressure in the evolution of segregated networks; this can also facilitate reduction of wiring and metabolism costs by limiting the number of long-distance connections used for integration of local networks^[19]. We hypothesized that abnormal visual experiences in HM subjects would lead to disrupting whole-brain functional connectivity hubs. Graph theory-based network analyses have recently been used to mirror functional connectivity within whole-brain networks^[20]. The degree centrality (DC) approach is a standard by which to measure the importance of the individual node; it reflects the properties of the functional brain network “hub” and exhibits comparatively high test-retest reliability^[21]. The DC method is currently drawing intense attention because it is the most reliable metric among several large-scale network metrics. This graph-based method measures functional relationships between a brain region and the rest of the brain within the entire connectivity matrix of the brain (connectome) at the voxel level^[22]. Because the DC method does not choose the regions of interests in

advance, the DC approach has been successfully used to evaluate brain network changes in many diseases such as depression^[23], obstructive sleep apnea^[24], and Alzheimer’s disease^[25].

Here, we aimed to investigate the centrality analysis through a graph-theoretical approach in HM patients using rs-fMRI data. We hypothesized that the degree of centrality changes might be used as an indicator for functional connectivity hubs changes in HM, which might reflect the neural substrate in HM patients.

SUBJECTS AND METHODS

Subjects A total of 38 right-handed patients with HM (17 males and 21 females) from the Ophthalmology Department of the First Affiliated Hospital of Nanchang University were enrolled in the study. All HM patients were vision corrected by glasses. The inclusion criteria of HM individuals were a binocular refractive diopter of -6.00 to -7.00 D and absence of any other ocular diseases (*e.g.* amblyopia, strabismus, glaucoma, cataracts, optic neuritis, retinal degeneration). The exclusion criteria of this study were myopia with a refractive diopter of -1.00 to -6.00 D; unilateral HM; HM with amblyopia and related complications (*e.g.* retinal atrophy degeneration, retinal detachment, macular hole); and psychiatric disorders and cerebral infarction diseases (the examination of myopia was conducted by two experienced ophthalmologist).

Thirty-eight right-handed healthy controls (HCs) with gender, age and educational level matching to the subjects in the HM group were also recruited for this study. The inclusion criteria were absence of any ocular disease with uncorrected visual acuity (VA) >1.0; absence of psychiatric disorders (*e.g.* depression, schizophrenia, vesania); and eligibility to MRI (*e.g.* no cardiac pacemaker, replacement heart valves or implanted metal devices).

The study was performed in accordance with both the Declaration of Helsinki and the medical ethics of the First Affiliated Hospital of Nanchang University. Importantly, it was approved by the First Affiliated Hospital of Nanchang University. All subjects provided written informed consent after receiving a full explanation of the purposes, methods, and potential risks of the study.

Magnetic Resonance Imaging Data Acquisition All MRI data were collected on a Siemens Trio 3.0T scanner by implementing an 8-channel head coil in the First Affiliated Hospital of Nanchang University, China. MRI scanning was performed on each subject. The whole-brain T1-weights were obtained with magnetization prepared gradient echo image (MPRAGE) with these parameters: repetition time =1900ms, echo time (TE) =2.26ms, thickness =1.0 mm, no intersection gap, acquisition matrix =256×256, field of view (FOV) =240×240 mm², flip angle =12°. Functional images were obtained by using gradient-echo-planar imaging sequence with the following

Table 1 Demographics and clinical measurements by group

Condition	HM	HC	<i>t</i>	<i>P</i> ^a
Male/female	17/21	17/21	N/A	>0.99
Age (y)	21.29±1.33	21.42±1.29	-0.438	0.663
Weight (kg)	66.05±5.93	65.82±6.15	0.171	0.865
Handedness	38R	38R	N/A	>0.99
Duration of HM (y)	7.26±1.00	N/A	N/A	N/A
Refractive diopter-right (D)	-6.52±0.34	N/A	N/A	N/A
Refractive diopter-left (D)	-6.53±0.33	N/A	N/A	N/A
Best-corrected VA-right eye	1.12±0.11	1.17±0.16	1.497	0.139
Best-corrected VA-left eye	1.15±0.13	1.16±0.15	-0.496	0.621

HM: High myopic; HC: Healthy control; N/A: Not applicable; D: Diopter; VA: Visual acuity. ^a*P*<0.05, statistically significant.

parameters: TR=2000ms, TE=40ms, flip angle =90°, slice thickness/gap=4.0/1 mm, FOV=240×240 mm², in-plane resolution=64×64, and 30 axial slices and 240 volumes were acquired in 8min. All subjects underwent the MRI scanning with eye closed without falling asleep.

Functional Magnetic Resonance Imaging Data Preprocessing

All the functional data were pre-filtered with MRIcro (www.MRIcro.com) and preprocessed using SPM8 (http://www.fil.ion.ucl.ac.uk/spm), DPARSFA (http://rfmri.org/DPARSA), and the Resting-state Data Analysis Toolkit (REST; http://www.restfmri.net). The following main step performed: 1) after removing the first 10 volumes in time, the rest of the 230 volumes were collected, and the head move was corrected; 2) slice-timing correction, motion correction, spatial realignment; 3) normalization [Montreal Neurological Institute 152 (MNI-152) space, Montreal, Canada], re-sampling as 3 mm³ cube voxels. The Diffeomorphic Anatomical Registration Through Exponentiated Lie Algebra (DARTEL) tool was used to compute the transformations from the individual native space to the MNI space and vice-versa. Finally, to further mitigate the influences of confounding factors, including signals from white matter and cerebrospinal fluid, whole-brain mean time series of all voxels was implemented; temporal filtering (0.01-0.1 Hz) was then performed. More details are described in our previous study^[24].

Degree Centrality Analysis Using an individual voxel-wise functional network, the number of significant suprathreshold correlations (or the degree of the binarized adjacency matrix) was counted for each subject; this permitted calculation of DC. Then, the following equation was used to convert each individual's voxel-wise DC map into a z-score map^[22].

Ophthalmic Testing Non-cycloplegic auto-refractometry (Topcon RM-A7000; Topcon Co., Tokyo, Japan) was carried out to measure the spherical equivalent (SE) in myopia subjects (SE=spherical power +1/2 cylindrical power). The device Zeiss IOL Master (Carl Zeiss Jena GmbH, Jena, Germany) was used to measure the axial length in all myopia subjects. The

macular foveal thickness of myopia was calculated by using the CIRRUS™ High-definition-OCT device (Zeiss). The VA of all subjects was measured applying the logMAR table.

Statistical Analysis For clinical features analysis: the independent sample *t*-test was used for comparisons of the duration of HM, axial length, macular foveal thickness and SE. Using the SPSS software version 16.0 (SPSS Inc., Chicago, IL, USA). Values of *P*<0.05 was considered statistically significant.

For DC analysis: the SPM8 toolkit was used to perform analysis with a general linear model (GLM) to assess group differences between HM patients and HCs, with respect to DC values. Gaussian random field (GRF) correction was used, and the significance level was set at *P*<0.05.

For brain-behavior correlation analysis: the associations between mean DC values in distinct brain regions and related clinical features in HM groups were assessed by using Pearson's correlation analysis (*P*<0.05 was considered statistically significant).

RESULTS

Demographics and Visual Measurements We did not find any significant differences in age (*P*=0.663), weight (*P*=0.865), best-corrected VA-right (*P*=0.139), and best-corrected VA-left (*P*=0.621) between the two groups. Furthermore, the mean values of the refractive diopter-right and the refractive diopter-left in HM were -6.52±0.34 D and -6.53±0.33 D, respectively; the mean values of the duration of HM was 7.26±1.00y (Table 1).

Degree Centrality Differences Compared with HCs, HM patients had significantly decreased DC values in the right inferior frontal gyrus (IFG)/insula, right middle frontal gyrus (MFG), and right supramarginal gyrus (SMG)/inferior parietal lobule (IPL; Figure 1A, 1B, blue and Table 2). In contrast, HM patients exhibited higher DC values in the right cerebellum posterior lobe, left precentral/postcentral gyrus (PreCG/PosCG), and right middle cingulate gyrus (Figure 1A, 1B, red and Table 2). The mean values of altered DC between the two groups are shown in Figure 1C. In the HM group, no

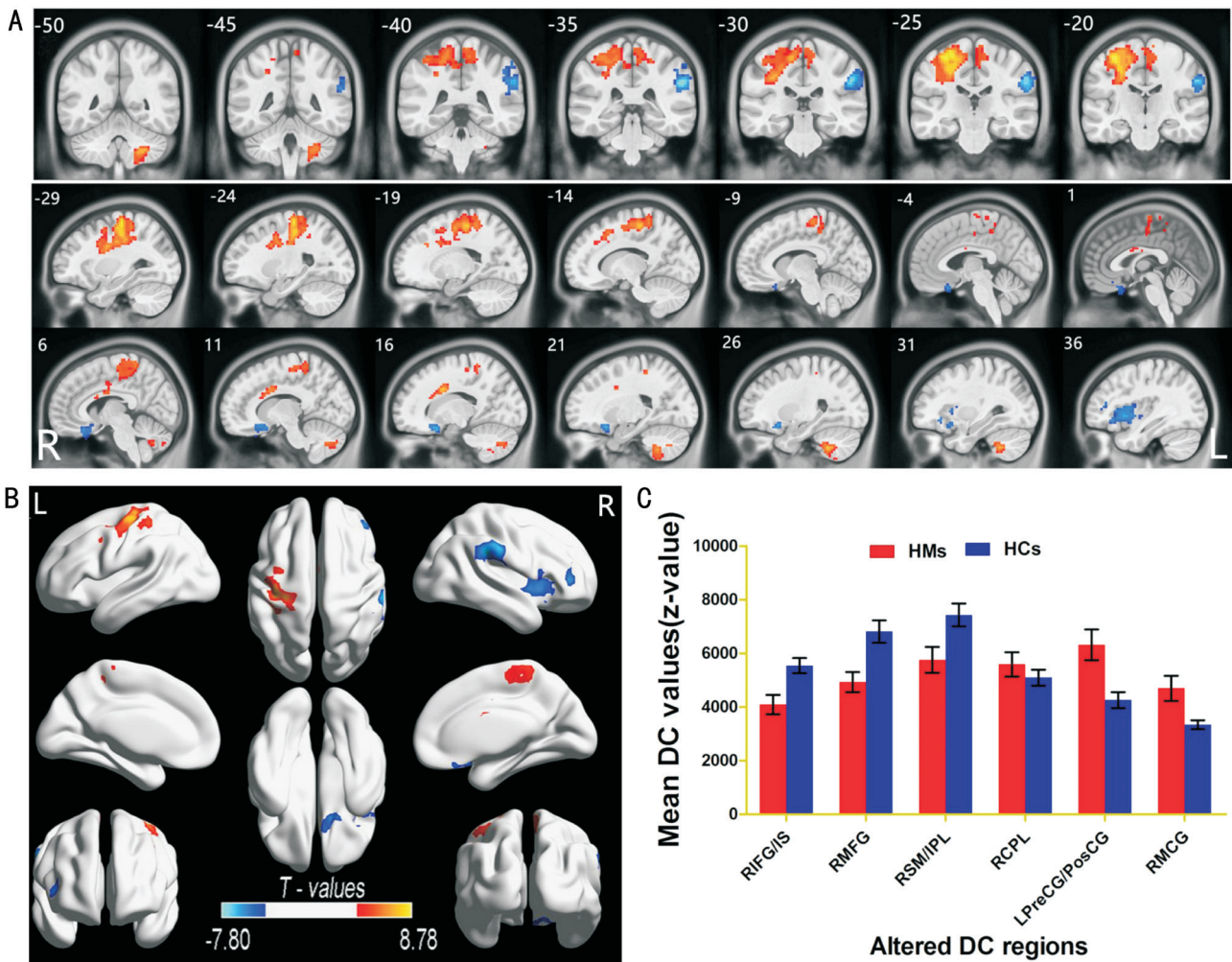


Figure 1 Spontaneous brain activities in HMs and HCs A, B: Significant activity differences were observed in the right IFG/insula, right MFG, and right SMG/IPL, and significantly increased DC values were observed in the right cerebellum posterior lobe, left PreCG/PosCG, and right MFG. Red or yellow areas denote higher DC values, and blue areas indicate lower DC values ($P < 0.01$ for multiple comparisons using GRF theory; $z > 2.3$, $P < 0.01$, cluster > 40 voxels, AlphaSim corrected); C: Mean values of altered DC values between the HM and HC groups.

Table 2 Brain areas with significantly different DC values between two groups

Brain areas	MNI coordinates			Voxels	BA	L/R	Peak T values
	x	y	z				
HM<HC							
Inferior frontal gyrus/ insula	33	30	-9	584	47,13,11	R	-6.171
Middle frontal gyrus	48	42	6	221	46,10	R	-6.292
Supramarginal /inferior parietal lobule	54	-33	33	335	40	R	-7.801
HM>HC							
Cerebellum posterior lobe	27	-48	-45	203		R	7.034
Precentral gyrus/ postcentral gyrus	-36	-21	60	1599	3,4,6	L	8.798
Middle cingulate gyrus	15	6	33	110	24	R	7.068

DC: Degree centrality; BA: Brodmann area; HM: High myopic; HC: Healthy control; MNI: Montreal neurological institute; L: Left; R: Right. The statistical threshold was set at the voxel level with $P < 0.05$ for multiple comparisons using Gaussian random field (GRF) theory ($z > 2.3$, $P < 0.01$, cluster > 40 voxels, AlphaSim corrected).

significant correlation was found between the mean DC values in the different brain regions and the clinical manifestations ($P > 0.05$).

Receiver Operating Characteristic Curve We speculated that the DC differences between the two groups might be

useful diagnostic markers. Thus, the mean DC values in the different brain regions were analyzed by the receiver operating characteristic (ROC) curve method. The areas under the ROC curve were as follows: right IFG/insula (0.778), right MFG (0.758), and right SMG/IPL (0.759) (HMs<HCs; Figure 2A);

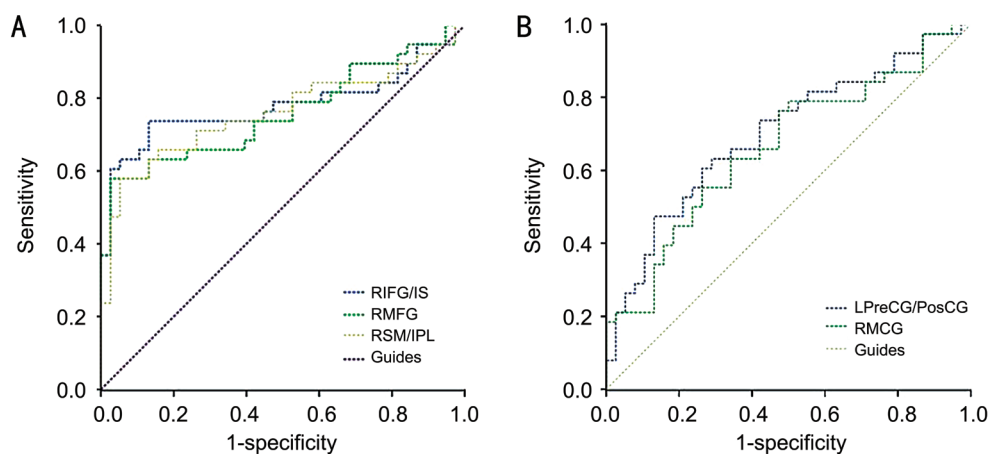


Figure 2 ROC curve analysis of the mean DC values for altered brain regions A: The areas under the ROC curve were 0.778 ($P < 0.001$; 95%CI: 0.664-0.892) for RIFG/IS; 0.758 ($P < 0.001$; 95%CI: 0.645-0.870) for RMFG; 0.759 ($P < 0.001$; 95%CI: 0.645-0.873) for RSM/IPL; (HMs < HCs); B: The areas under the ROC curve were 0.699 ($P = 0.003$; 95%CI: 0.580-0.817) for LPreCG/PosCG; 0.663 ($P = 0.015$; 95%CI: 0.540-0.785) for RMCG (HMs > HCs).

left PreCG/PosCG (0.699) and right middle cingulate gyrus (0.663) (HMs > HCs; Figure 2B).

DISCUSSION

In our study, we evaluated the network centrality difference between HM and HC groups. We found that HM patients exhibited significant reductions in DC values in the right IFG/insula, right SMG/IPL, and right MFG. In contrast, HM patients exhibited significant reductions in DC values in the left PreCG/PosCG, right cerebellum posterior lobe, and right middle cingulate gyrus.

Analysis of Decreased Degree Centrality in High Myopia Our results demonstrated that HM patients showed significantly lower DC in insula. The insula is involved in visceral sensory and somatic sensory processes; notably, it comprises functionally heterogeneous brain region. In a study of the ventral-anterior and dorsal-posterior insula, Cauda *et al*^[26] revealed two major complementary networks, suggesting a role for the insula with regard to emotional aspects and sensorimotor integration. Moreover, the insula was the core hub of salience network^[27] and visuomotor integration network^[28]. HM patients exhibited significant reductions in DC values in the insula, indicating disturbance of the salience and visuomotor integration networks. Thus, we speculated that the abnormal visual experience in HM might lead to the dysfunction of visuomotor integration network.

The IFG lies within the frontal lobe, and is important in language processing^[29]. Furthermore, the English subjects showed increased activity in the left IFG with linguistic experience work^[30]. The IFG is a critical node of the brain's language network^[31]. Furthermore, the IFG is associated with inhibition and attentional control^[32]. In a previous study, we revealed lower amplitude of low-frequency fluctuation values in the right IFG of HM patients^[17]. Additionally, we found that significant reduction of DC values in the right IFG of

HM patients, which may indicate IFG dysfunction. Thus, we speculated that HM might be involved in the impairment of language understanding.

The middle frontal gyrus (MFG) represents a considerable portion of the frontal lobe, and is important in working memory^[33]. Furthermore, the MFG is associated with contingency awareness^[34]. The MFG is the highest terminal of the parieto-prefrontal pathway^[35] and has direct connections with the IPL and middle temporal gyrus^[36-37]. The MFG is involved in top-down control of visual-spatial processing, such as spatial attention and working memory^[38]. A previous study showed comparably smaller white matter in the prefrontal lobe of HM patients^[16]. Consistent with these findings, we found significant reduction in DC values in the right MFG of HM patients, which might indicate deficits of visual-spatial processing in the HM group.

The SMG/IPL is a part of the parietal lobe, which is known as Brodmann area 40. The SMG plays an important role in the phonological understanding^[39-40]. Furthermore, the SMG is involved in the visual word recognition^[41]. A recent study revealed reduction in the density of long-range functional connectivity in the SMG of HM patients^[18]. The IPL is important in visual-motor integration, which is the core hub involved in correlation of the visual and motor networks. We also revealed significant reductions in DC values in the right SMG/IPL of HM patients, suggesting dysfunction of the visual-motor network in HM patients.

The Analysis of Increased Degree Centrality in High Myopia

The primary motor cortex (Brodmann area 4) is located within the PreCG. The PreCG is located in front of the PosCG. The PreCG and PosCG comprise the core hub of the sensorimotor network (SMN). The primary motor cortex is important in action encoding^[42]. Furthermore, PreCG is involved in oculomotor and somatomotor space processing^[43] and the

motor hand area^[44]. In addition, PosCG is the location of the primary somatosensory cortex, which is responsible for the sense of touch^[45]. Our results showed that significant increased DC in PreCG and PosCG were observed in the HM patients, indicating reorganization of SMN in HM patients.

The cingulate gyrus comprises the limbic cortex hub, and participates in the control of pain and emotion^[46]. Dysfunction of the cingulate gyrus is linked to a number of diseases, including depression^[47], schizophrenia^[48], Alzheimer's disease^[49], and others. In our study, increased DC was present in the cingulate gyrus of HM patients, which suggests reorganization of the limbic system.

In summary, we found altered DC in various brain regions occurred in HM patients which might indicate the reorganization of visuomotor integration network and sensorimotor network and limbic system in HM patients.

Limitation and Future Recommendations There some limitations in this study. The first limitation is the small sample size. The second limitation is that HMs subjects do not underwent psychological tests. The third limitation is that, although all participants underwent the fMRI without any task, the DC signals would still be affected by physiological noise (*i.e.* by cardiac and respiratory activity). The diopter of myopia subject is -6.00 to -7.00 D. In future study, we would enlarge the sample size. Various neurophysiological scales were conducted to assess the behavioral and physiological changes in HM patients. Multimodal MRI technologies will be used to determine the functional and morphological changes in HM patients.

ACKNOWLEDGEMENTS

Foundations: Supported by National Natural Science Foundation of China (No.81760179; No.81360151); Natural Science Foundation of Jiangxi Province (No.20171BAB205046); Jiangxi Province Education Department Key Foundation (No. GJJ160033); Health Development Planning Commission Science Foundation of Jiangxi Province (No.20185118).

Conflicts of Interest: Hu YX, None; He JR, None; Yang B, None; Huang X, None; Li YP, None; Zhou FQ, None; Xu XX, None; Zhong YL, None; Wang J, None; Wu XR, None.

REFERENCES

- 1 Holden BA, Fricke TR, Wilson DA, Jong M, Naidoo KS, Sankaridurg P, Wong TY, Naduvilath TJ, Resnikoff S. Global prevalence of myopia and high myopia and temporal trends from 2000 through 2050. *Ophthalmology* 2016;123(5):1036-1042.
- 2 Wong Y, Saw S. Epidemiology of Pathologic Myopia in Asia and Worldwide. *Asia Pac J Ophthalmol* 2016;5(6):394-402.
- 3 Lichtwitz O, Boissonnot M, Mercié M, Ingrand P, Leveziel N. Prevalence of macular complications associated with high myopia by multimodal imaging. *J Fr Ophthalmol* 2016;39(4):355-363.
- 4 Ikuno Y, Fujimoto S, Jo Y, Asai T, Nishida K. Choroidal thinning in high myopia measured by optical coherence tomography. *Clin Ophthalmol*

- 2013;7:889-893.
- 5 Alkabes M, Burés-Jelstrup A, Salinas C, Medeiros MD, Rios J, Corcostegui B, Mateo C. Macular buckling for previously untreated and recurrent retinal detachment due to high myopic macular hole: a 12-month comparative study. *Graefes Arch Clin Exp Ophthalmol* 2014;252(4):571-581.
- 6 Wang P, Liu X, Ye Z, Gong B, Yang Y, Zhang D, Wu X, Zheng H, Li Y, Yang Z, Shi Y. Association of IGF1 and IGF1R gene polymorphisms with high myopia in a Han Chinese population. *Ophthalmic Genet* 2017;38(2):122-126.
- 7 Jonas JB, Xu L, Wang YX, *et al.* Education-Related parameters in high myopia: adults versus school children. *PLoS One* 2016;11(5):e0154554.
- 8 Ramamurthy D, Lin Chua SY, Saw SM. A review of environmental risk factors for myopia during early life, childhood and adolescence. *Clin Exp Optom* 2015;98(6):497-506.
- 9 Hashemi H, Miraftab M, Ghaffari R, Asgari S. Femtosecond-assisted lasik versus prk: comparison of 6-month visual acuity and quality outcome for high myopia. *Eye Contact Lens* 2016;42(6):354-357.
- 10 Kohnen T, Maxwell WA, Holland S. Correction of moderate to high myopia with a foldable, angle-supported phakic intraocular lens: results from a 5-year open-label trial. *Ophthalmology* 2016;123(5):1027-1035.
- 11 Malakar M, Askari SN, Ashraf H, Waris A, Ahuja A, Asghar A. Optical coherence tomography assisted retinal nerve fibre layer thickness profile in high myopia. *J Clin Diagn Res* 2015;9(2):NC01-3.
- 12 Yang Y, Wang J, Jiang H, Yang X, Feng L, Hu L, Wang L, Lu F, Shen M. Retinal microvasculature alteration in high myopia. *Invest Ophthalmol Vis Sci* 2016;57(14):6020-6030.
- 13 Moriyama M, Ohno-Matsui K, Modegi T, Kondo J, Takahashi Y, Tomita M, Tokoro T, Morita I. Quantitative analyses of high-resolution 3D MR images of highly myopic eyes to determine their shapes. *Invest Ophthalmol Vis Sci* 2012;53(8):4510-4518.
- 14 Moriyama M, Ohno-Matsui K, Hayashi K, Shimada N, Yoshida T, Tokoro T, Morita I. Topographic analyses of shape of eyes with pathologic myopia by high-resolution three-dimensional magnetic resonance imaging. *Ophthalmology* 2011;118(8):1626-1637.
- 15 Mirzajani A, Sarlaki E, Kharazi HH, Tavan M. Effect of lens-induced myopia on visual cortex activity: a functional MR imaging study. *AJNR Am J Neuroradiol* 2011;32(8):1426-1429.
- 16 Li Q, Guo M, Dong H, Zhang Y, Fu Y, Yin X. Voxel-based analysis of regional gray and white matter concentration in high myopia. *Vis Res* 2012;58:45-50.
- 17 Huang X, Zhou FQ, Hu YX, Xu XX, Zhou X, Zhong YL, Wang J, Wu XR. Altered spontaneous brain activity pattern in patients with high myopia using amplitude of low-frequency fluctuation: a resting-state fMRI study. *Neuropsychiatr Dis Treat* 2016;12:2949-2956.
- 18 Zhai L, Li Q, Wang T, Dong H, Peng Y, Guo M, Qin W, Yu C. Altered functional connectivity density in high myopia. *Behav Brain Res* 2016;303:85-92.
- 19 Bassett DS, Bullmore ET. Small-world brain networks revisited. *Neuroscientist* 2017;23(5):499-516.
- 20 Wang J, Zuo X, He Y. Graph-based network analysis of resting-state functional MRI. *Front Syst Neurosci* 2010;4:16.

Degree centrality study in high myopia patients

- 21 Zuo XN, Xing XX. Test-retest reliabilities of resting-state fMRI measurements in human brain functional connectomics: a systems neuroscience perspective. *Neurosci Biobehav Rev* 2014;45:100-118.
- 22 Zuo XN, Ehmke R, Mennes M, Imperati D, Castellanos FX, Sporns O, Milham MP. Network centrality in the human functional connectome. *Cereb Cortex* 2012;22(8):1862-1875.
- 23 Gao C, Wenhua L, Liu Y, Ruan X, Chen X, Liu L, Yu S, Chan RC, Wei X, Jiang X. Decreased Subcortical and increased cortical degree centrality in a nonclinical college student sample with subclinical depressive symptoms: a resting-state fMRI study. *Front Hum Neurosci* 2016;10:617.
- 24 Li H, Li L, Shao Y, Gong H, Zhang W, Zeng X, Ye C, Nie S, Chen L, Peng D. Abnormal intrinsic functional hubs in severe male obstructive sleep apnea: evidence from a voxel-wise degree centrality analysis. *PLoS One* 2016;11(10):e164031.
- 25 Guo Z, Liu X, Hou H, Wei F, Liu J, Chen X. Abnormal degree centrality in Alzheimer's disease patients with depression: a resting-state functional magnetic resonance imaging study. *Exp Gerontol* 2016;79:61-66.
- 26 Cauda F, D'Agata F, Sacco K, Duca S, Geminiani G, Vercelli A. Functional connectivity of the insula in the resting brain. *Neuroimage* 2011;55(1):8-23.
- 27 Uddin LQ. Salience processing and insular cortical function and dysfunction. *Nat Rev Neurosci* 2015;16(1):55-61.
- 28 Burgess CR, Livneh Y, Ramesh RN, Andermann ML. Gating of visual processing by physiological need. *Curr Opin Neurobiol* 2018;49:16-23.
- 29 Rota G, Sitaram R, Veit R, Erb M, Weiskopf N, Dogil G, Birbaumer N. Self-regulation of regional cortical activity using real-time fMRI: the right inferior frontal gyrus and linguistic processing. *Hum Brain Mapp* 2009;30(5):1605-1614.
- 30 Hsieh L, Gandour J, Wong D, Hutchins GD. Functional heterogeneity of inferior frontal gyrus is shaped by linguistic experience. *Brain Lang* 2001;76(3):227-252.
- 31 Acheson DJ, Hagoort P. Stimulating the brain's language network: syntactic ambiguity resolution after TMS to the inferior frontal gyrus and middle temporal gyrus. *J Cogn Neurosci* 2013;25(10):1664-1677.
- 32 Hampshire A, Chamberlain SR, Monti MM, Duncan J, Owen AM. The role of the right inferior frontal gyrus: inhibition and attentional control. *Neuroimage* 2010;50(3):1313-1319.
- 33 Olesen PJ, Westerberg H, Klingberg T. Increased prefrontal and parietal activity after training of working memory. *Nat Neurosci* 2004;7(1):75-79.
- 34 Carter RM, O'Doherty JP, Seymour B, Koch C, Dolan RJ. Contingency awareness in human aversive conditioning involves the middle frontal gyrus. *Neuroimage* 2006;29(3):1007-1012.
- 35 Schall JD, Morel A, King DJ, Bullier J. Topography of visual cortex connections with frontal eye field in macaque: convergence and segregation of processing streams. *J Neurosci* 1995;15(6):4464-4487.
- 36 Clower DM, Dum RP, Strick PL. Basal ganglia and cerebellar inputs to 'AIP'. *Cereb Cortex* 2005;15(7):913-920.
- 37 Sakata H, Kusunoki M. Organization of space perception: neural representation of three-dimensional space in the posterior parietal cortex. *Curr Opin Neurobiol* 1992;2(2):170-174.
- 38 Friedman HR, Goldman-Rakic PS. Coactivation of prefrontal cortex and inferior parietal cortex in working memory tasks revealed by 2DG functional mapping in the rhesus monkey. *J Neurosci* 1994;14(5 Pt 1):2775-2788.
- 39 Hartwigsen G, Baumgaertner A, Price CJ, Koehnke M, Ulmer S, Siebner HR. Phonological decisions require both the left and right supramarginal gyri. *Proc Natl Acad Sci U S A* 2010;107(38):16494-16499.
- 40 Sliwinska MW, Khadilkar M, Campbell-Ratliff J, Quevenco F, Devlin JT. Early and sustained supramarginal gyrus contributions to phonological processing. *Front Psychol* 2012;3:161.
- 41 Stoeckel C, Gough PM, Watkins KE, Devlin JT. Supramarginal gyrus involvement in visual word recognition. *Cortex* 2009;45(9):1091-1096.
- 42 Hari R, Forss N, Avikainen S, Kirveskari E, Salenius S, Rizzolatti G. Activation of human primary motor cortex during action observation: a neuromagnetic study. *Proc Natl Acad Sci U S A* 1998;95(25):15061-15065.
- 43 Iacoboni M, Woods RP, Lenzi GL, Mazziotta JC. Merging of oculomotor and somatomotor space coding in the human right precentral gyrus. *Brain* 1997;120(Pt 9):1635-1645.
- 44 Yousry TA, Schmid UD, Alkadhi H, Schmidt D, Peraud A, Buettner A, Winkler P. Localization of the motor hand area to a knob on the precentral gyrus. A new landmark. *Brain* 1997;120(Pt 1):141-157.
- 45 Ebisch SJ, Perrucci MG, Ferretti A, Del GC, Romani GL, Gallese V. The sense of touch: embodied simulation in a visuotactile mirroring mechanism for observed animate or inanimate touch. *J Cogn Neurosci* 2008;20(9):1611-1623.
- 46 Vogt BA. Pain and emotion interactions in subregions of the cingulate gyrus. *Nat Rev Neurosci* 2005;6(7):533-544.
- 47 Ebert D, Ebmeier KP. The role of the cingulate gyrus in depression: from functional anatomy to neurochemistry. *Biol Psychiatry* 1996;39(12):1044-1050.
- 48 Haznedar MM, Buchsbaum MS, Hazlett EA, Shihabuddin L, New A, Siever LJ. Cingulate gyrus volume and metabolism in the schizophrenia spectrum. *Schizophr Res* 2004;71(2-3):249-262.
- 49 Jones BF, Barnes J, Uylings HB, Fox NC, Frost C, Witter MP, Scheltens P. Differential regional atrophy of the cingulate gyrus in Alzheimer disease: a volumetric MRI study. *Cereb Cortex* 2006;16(12):1701-1708.